The Effect of Minor Components on Milk Fat Crystallization

Amanda J. Wright[a], Richard W. Hartel[b], Suresh S. Narine[a], and Alejandro G. Marangoni[a,*]

Departments of [a]Food Science, University of Guelph, Ontario Canada N1G 2W1, and [b]Food Science, University of Wisconsin-Madison, Madison, Wisconsin 53706

ABSTRACT: Milk fat is composed of 97–98% triacylglycerols and 2–3% minor polar lipids. In this study triacylglycerols were chromatographically separated from minor components. Isolated diacylglycerols from the polar fraction were also added back to the milk fat triacylglycerols. The crystallization behaviors of native anhydrous milk fat (AMF), milk fat triacylglycerols (MF-TAG), and milk fat triacylglycerols with diacylglycerols added back (MF-DAG) were studied. Removal of minor components and addition of diacylglycerols had no effect on dropping points or equilibrium solid fat contents. Presence of the minor components, however, did delay the onset of crystallization at low degrees of supercooling. Crystallization kinetics were quantified using the Avrami model. Sharp changes in the values of the Avrami constant *k* and exponent *n* were observed for all three fats around 20.0°C. Increases in *n* around 20.0°C indicated a change from one-dimensional to multidimensional growth. Differences in *k* and *n* of MF-DAG from AMF and MF-TAG suggested that the presence of milk fat diacylglycerols changes the crystal growth mechanism. Apparent free energies of nucleation ($\Delta G_{c,\text{apparent}}$) were determined using the Fisher-Turnbull model. $\Delta G_{c,\text{apparent}}$ for AMF was significantly greater than $\Delta G_{c,\text{apparent}}$ for MF-TAG, and $\Delta G_{c,\text{apparent}}$ for MF-DAG was significantly less than those for both AMF and MF- TAG. The microstructural networks of AMF, MF-TAG, and MF-DAG, however, were similar at both 5.0 and 25.0°C, and all three fats crystallized into the typical β′-2 polymorph. Differential scanning calorimetry in both the crystallization and melting modes revealed no differences between the heat flow properties of AMF, MF-TAG, and MF-DAG.

Paper no. J9401 in *JAOCS 77,* 463–475 (May 2000).

KEY WORDS: Avrami equation, crystallization, minor components, milk fat.

Triacylglycerols generally constitute 93–98% of the total lipid mass in fats and oils. The balance is composed mainly of polar lipid species such as partial acylglycerols, free fatty acids, and phospholipids. The influence of these minor lipids on fat crystallization has intrigued academic and industrial researchers concerned with fats for decades. Historically, polar lipids and other surface-active compounds have been used to manipulate fat crystallization. Butter manufacturers have long considered the possibility of using additives, including monoacylglycerols, to improve spreadability and decrease hardness (1–4). Similarly, the chocolate industry has used emulsifiers to stabilize preferred crystal polymorphs in cocoa butter (5). Oil processors have added partial acylglycerols to salad oils to prevent the formation of crystal sediments and cloudiness during cold storage (6). The stabilizing influence of minor components on less stable polymorphic crystal forms has been especially well documented (7). For example, Hernqvist and Anjou (8) showed that diacylglycerols cocrystallize with rapeseed triacylglycerols in margarines and stabilize the β′ crystal polymorph, delaying the transformation to the less desirable, but thermodynamically more stable, β form.

One of the earliest studies published in this area was carried out by the French researcher Loncin in 1958 (9). Loncin investigated the effect of partial glycerols on palm oil plasticity. He concluded that palm oils high in free fatty acids tend to have lower melting points because of the formation of eutectics between the triacylglycerols and the diacylglycerols that are present (9). Diacylglycerols have since been shown either to enhance or to retard crystallization in palm oil, depending on their compatibility with the surrounding triacylglycerols. Dipalmitoylglycerol caused rapid palm olein crystallization, palmitoyloleoylglycerol retarded crystallization, and dioleoylglycerol had no significant effect (10). Similarly, in coconut oil triacylglycerols, dilauroylglycerol retarded nucleation, but dioleoylglycerol had no significant effect (11). Cebula and Smith (12) reported that diacylglycerols in Coberine (a cocoa butter equivalent) reduce the fat's crystallization induction time but subsequently slow down the velocity of growth (12). In cocoa butter, Davis and Dimick (13,14) found that the surface-active properties of complex lipids, including glycolipids and phospholipids, influenced the formation of stable seed crystals by forming the bulk of the nucleus and aiding in the preferential incorporation of trisaturated glycerols. Similar research has been conducted on a number of different fats and oils by several researchers. In particular, Niiya *et al.* (15,16), Reddy *et al.* (17), and Riiner (18) have made significant contributions.

The case for milk fat crystallization has also been touched upon. Addition of 1% milk fat monoacylglycerols to milk fat triacylglycerols increased the fat's spreadability (19). How-

*To whom correspondence should be addressed at Department of Food Science, University of Guelph, Ontario, Canada N1G-2WI.
E-mail: amarango@foodsci.uoguelph.ca

ever, while monoacylglycerols did temporarily decrease butter's hardness, the effect disappeared upon extended storage (3). King (1) could find no consistent relationship between the chemical structure of minor lipids added to milk fat triacylglycerols and their resulting effects on physical properties.

Clearly, the relationship between minor components and fat crystallization is complicated. Despite many efforts, there remains little agreement about the nature of the minor components' effects. Our group is interested in resolving the issue for milk fat in particular. This work seeks first to characterize the effect of milk fat's minor components on crystallization behavior. The effect on milk fat structure will be pursued at a later stage.

MATERIALS AND METHODS

Separation of milk fat into the milk fat triacylglycerols (MF-TAG) and minor lipids. Anhydrous milk fat (AMF) was separated based on the method originally described by Carroll (20), using Florisil (activated magnesium silicate), into two fractions: the MF-TAG and minor lipid components. The MF-TAG were eluted with 20:80 diethyl ether/hexane and subsequently the bound, more polar lipids were eluted with methanol. Purity of the MF-TAG and minor lipid fractions was verified by thin-layer chromatography (TLC) on silica plates impregnated with boric acid using 96:4 (vol/vol) chloroform/acetone (21).

Characterization of AMF, MF-TAG, and minor polar lipids. Fatty acid analysis of AMF and the MF-TAG was performed by gas-liquid chromatography (GLC) according to the method of Bannon *et al*. (22). Triacylglycerol compositions of the two fats were determined by GLC as previously described (23). Diacylglycerol and monoacylglycerol isomers and free fatty acids were detected using TLC by comparing to Sigma (St. Louis, MO) standards. Cholesterol and cholesterol esters, glycolipids, and phospholipids were colorimetrically detected in the methanol fraction on TLC plates with spray reagents (Sigma Chemical Co.). Cholesterol and cholesterol esters were identified with ferric chloride, glycolipids with Bial's reagent containing orcinol ferric chloride, and phospholipids with the molybdenum blue spray reagent containing molybdenum oxide (1.3%) in 4.2 M sulfuric acid.

The polar fraction was analyzed by gas chromatography–mass spectroscopy using the VG Trio-1000 benchtop quadrupole mass spectrometer (VG-MICROMASS, Manchester, England), which was operated by the LAB-BASE data system software supplied with the VG Trio-1000. The equipment was run in electron ionization mode with an accelerating potential of 70 volts. A 30-m DB wax column was used. The temperature was initially held at 60°C for 2 min then ramped to 180°C at 5°C/min, at which point it was held for 30 min. The injector temperature was 200°C. The Dynolite detector looked at masses between 40 and 460 atomic mass units.

Collection and characterization of milk fat diacylglycerols. Milk fat diacylglycerols were recovered from the methanol fraction by scraping TLC plates. The lipids were recovered from the silica by vigorous vortexing in 2:1 chloroform/methanol. Fatty acid analysis of the diacylglycerols was performed as above, and the positional distribution was calculated after determining the composition of the 1,2/2,3- and 1,3-diacylglycerol bands individually. The diacylglycerols were added to the MF-TAG at the 0.1 wt% level with heat and vigorous vortexing. MF-TAG with the diacylglycerol addition will be referred to as MF-DAG.

Characterization of AMF, MF-TAG, and MF-DAG crystallization behavior. Dropping points were determined according to Rousseau *et al*. (23). The crystallization behavior of the AMF, MF-TAG, and MF-DAG was studied by following the development of solid fat. Solid fat content (SFC) was measured by pulsed nuclear magnetic resonance (pNMR) with a Bruker PC20 Series NMR analyzer (Bruker, Milton, Canada), according to the AOCS official method Cd 16-81 (24). Samples were heated at 80°C for 30 min before analysis to destroy any crystal history. Three replicates of each sample were then placed in a thermostated water bath, and SFC readings were taken at appropriate time intervals. Static crystallization was followed in this way at 5.0, 10.0, 15.0, 20.0, 22.5, 25.0, and 27.5°C. Induction times of crystallization (τ_{SFC}) were determined from curves of SFC as a function of time by extrapolating back to the onset time of the linear SFC increase. The crystallization curves were fitted to the Avrami equation by least squares nonlinear regression (25). The Avrami equation (26–28) can be used to quantify crystallization kinetics and give an indication of the nature of the crystal growth process; that is,

$$\frac{\mathrm{SFC}(t)}{\mathrm{SFC}(\infty)} = 1 - e^{-kt^n} \qquad [1]$$

where SFC(t) describes the SFC as a function of time, SFC(∞) is the limiting SFC as time approaches infinity, k is the Avrami constant, and n is the Avrami exponent.

The equation was developed to study the kinetics of phase change, and its principles were first applied to polymer crystallization in the 1950s. Researchers have used the Avrami model in the study of fat crystallization (29–33). The equation describes an event in which there is an initial lag-period, where crystallization occurs very slowly, and a subsequent rapid increase in crystal mass (26). Avrami's theory takes into account that crystallization occurs by both nucleation and crystal growth (34) and is based on the assumptions of isothermal transformation conditions, spatially random nucleation, and linear growth kinetics in which the growth rate of the new phase depends only on temperature and not time (35).

The Avrami parameters provide information on the nature of the crystallization process. The constant k represents a crystallization rate constant. It depends primarily on the crystallization temperature (33) and generally follows an Arrhenius-type temperature dependency (36). The constant k takes both the nucleation and crystal growth rates into account (37). Half times of crystallization, $t_{1/2}$, reflect the magnitudes of the

rate constants according to the following relationship:

$$t_{1/2} = \left(\frac{0.693}{k}\right)^{1/n} \quad [2]$$

The Avrami exponent, *n*, sometimes referred to as an index of crystallization, indicates the crystal growth mechanism. This parameter is a combined function of the time dependence of nucleation and the number of dimensions in which growth takes place (37). Nucleation is either instantaneous, with nuclei appearing all at once early on in the process, or sporadic, with the number of nuclei increasing linearly with time (37). Growth occurs as either rods, discs, or spherulites in one, two, or three dimensions, respectively (33). Table 1 shows the value of the Avrami exponent, *n*, expected for various types of nucleation and growth.

Changes in optical density at 500 nm during crystallization were evaluated using a Beckman DU 7400 Spectrophotometer (Beckman Instruments, Mississauga, Canada). One gram of fat, heated at 80°C for 30 min, was statically crystallized at 15.0, 20.0, 22.5, 25.0, and 27.5°C in a temperature-controlled cell. The first derivative of each curve was taken to obtain the induction time ($\tau_{turbidity}$), which is the onset time of linear turbidity development. From these induction times, apparent activation free energies of nucleation (ΔG_c) were calculated according to the Fisher-Turnbull equation (38):

$$J = (NkT/h)\exp(-\Delta G_d/kT)\exp(-\Delta G_c/kT) \quad [3]$$

where *J* is the rate of nucleation and is inversely proportional to the induction time (τ) of nucleation, *N* is the number of molecules per cm^3 in liquid phase, *k* is the gas constant per molecule, *T* is the temperature (degrees K), *h* is Planck's constant, and ΔG_d is the activation free energy of diffusion. ΔG_c is the activation free energy of nucleation and, for a spherical nucleus, is related to the surface free energy of the crystal/liquid melt interface (σ) and the degree of supercooling (ΔT) according to the following relationship (38):

$$\Delta G_c = (16/3)\pi\sigma^3 T_m^2/(\Delta H)^2(\Delta T)^2 \quad [4]$$

where ΔH is the enthalpy of nucleation. The calculations were performed as described previously (39). Briefly, a plot of $\ln(\tau T)$ vs. $1/T(\Delta T)^2$ yields a slope (*m*) and permits calculation of the activation free energy of nucleation according to the following equation:

$$\Delta G_c = mk/(T_m - T)^2 \quad [5]$$

where T_m is the melting point and *T* is the crystallization temperature. Mettler dropping points were used for T_m.

To determine the polymorphic state of the AMF, MF-TAG, and MF-DAG crystals, powder X-ray diffraction spectroscopy was carried out using an Enraf-Nonius KappaCCD diffractometer (Nonius, Delft, The Netherlands) with an FR590 X-ray generator at 5.0 and 25.0°C. The d-spacings were calculated by comparing the spacing of the rings in these images to those of a standard ($CaSO_4 \cdot 2H_2O$).

Differential scanning calorimetry (DSC) of AMF, the MF-TAG, and the MF-DAG was performed in the crystallization and melting modes using a DuPont 1090 differential scanning calorimeter (Wilmington, DE). DSC pans with 7–10 mg of sample were heated for 10 min at 80°C and crystallized at a rate of 5°C/min from 60 to –40°C. Samples crystallized at 5°C for 24 h were melted from 5 to 60°C at 5°C/min.

An Olympus BH polarized light microscope (Olympus, Tokyo, Japan) was used to observe fat microstructure of AMF, the MF-TAG, and the MF-DAG after 5 d. Samples were crystallized from the melt on glass slides under glass coverslips at 5 and 25°C. A CCD digital video camera (Efston Science Inc., Toronto, Canada) was used to record images on videotape which were then digitized using Rainbow Runner software (Matrox Graphics Inc., Dorval, Québec, Canada).

Three-photon fluorescence microscopy was used to visualize AMF and the MF-TAG crystallized for 24 h at 20°C on a glass microscope slide under a cover slip as described by Marangoni and Hartel (40). The sample was excited at a wavelength of 1,047 nm.

TABLE 1
Values for the Avrami Exponent, *n*, for Different Types of Nucleation and Growth[a]

n	Type of crystal growth and nucleation expected
3 + 1 = 4	Spherulitic growth from sporadic nuclei
3 + 0 = 3	Spherulitic growth from instantaneous nuclei
2 + 1 = 3	Disc-like growth from sporadic nuclei
2 + 0 = 2	Disc-like growth from instantaneous nuclei
1 + 1 = 2	Rod-like growth from sporadic nuclei
1 + 0 = 1	Rod-like growth from instantaneous nuclei

[a]After Reference 37.

RESULTS AND DISCUSSION

MF-TAG represented 97.1 wt% of the total mass in AMF (Table 2). This agrees well with previous reports that milk fat generally contains somewhere between 96 and 98 wt% triacylglycerols (21,41,42). The minor components accounted for nearly 3 wt% of the AMF, also a reasonable figure based on previous reports. Milk fat's typical minor lipids were detected in the more polar fraction (Table 2).

Upon fractionation the yellow color of the native AMF appeared in the minor components fraction, but the MF-TAG appeared white. Figure 1 shows the three-photon excitation fluorescence micrographs of AMF and the MF-TAG. AMF contains an autofluorescent compound that cocrystallizes within the solid TAG crystal network (Fig. 1A). In the MF-TAG, removal of the minor components results in a lack of the autofluorescence (Fig. 1B). Preliminary research in our laboratory suggests that this autofluorescent compound is a carotenoid, possibly annatto, the yellowish β-carotene pigment added to milk fat during butter manufacture. This is supported by the fact that annatto was tentatively identified

TABLE 2
Reported (A, B, and C) and Experimentally Determined Composition of Milk Fat

	Composition (wt%)			
	A[a]	B[a]	C[a]	Experimental results
Triacylglycerols				
MF-TAG	97.50	95.8	97–98	97.10
Minor polar lipids	2.50	4.2	2–3	2.90
Diacylglycerols	0.360	2.25*	0.28–0.59[b]	Detected
Monoacylglycerols	0.027	0.08	0.16–0.38	Detected
Cholesterol esters	Trace	0.02	—	Detected
Cholesterol	0.310	0.46	0.419	Detected
Phospholipids	0.596	1.11	0.2–1.00	Detected
Glycolipids	Trace	NR	—	Detected
Free fatty acids	NR	0.28	0.10–0.44	Detected

[a]A: Reference 21; B: Reference 41; C: Reference 22.
[b]1,2-Diacylglycerol (21, 41, and 42). Abbreviation: MF-TAG, milk fat triacylglycerol; NR, not reported.

by GC–MS in the minor components fraction (results not shown).

Tables 3 and 4 show the fatty acid and triacylglycerol compositions, respectively, of AMF and the MF-TAG determined by GLC. AMF and MF-TAG had very similar fatty acid and triacylglycerol compositions. Removal of the minor components did not affect the overall chemical composition of the bulk material (the TAG). This is significant because it verifies that during the separation procedure the TAG were not themselves fractionated.

Mettler dropping points of AMF, MF-TAG, and MF-DAG were 34.0 ± 0.2, 33.8 ± 0.2, and 34.2 ± 0.2°C, respectively. Removal of the minor components and addition of diacylglycerols back to MF-TAG did not significantly affect the dropping point ($P > 0.05$). Therefore, the thermodynamic driving force behind crystallization is the same for AMF, MF-TAG, and MF-DAG in subsequent crystallization experiments because the degree of supercooling is the same in all three systems. The SFC vs. temperature profiles of AMF, MF-TAG, and MF-DAG are shown in Figure 2. The curves are identical; the same amount of solid fat is present in all three fats between 0 and 40°C. Milk fat minor components do not seem to alter the thermodynamics of the system since dropping points and the equilibrium SFC remain unchanged despite their removal. These results support research by van den Tempel (6), which found that minor surface-active lipids will not change the equilibrium SFC of a fat. Van den Tempel suggested, however, that crystallization kinetics may be altered (6).

The effects of milk fat minor components on crystallization kinetics are shown in Figures 3 and 4. The increase in SFC with time during static crystallization was followed at 5.0, 10.0, 15.0 (Fig. 3A–C) and 20.0, 22.5, 25.0, and 27.5°C (Fig. 4A–D). Minor components had an inhibitory effect on

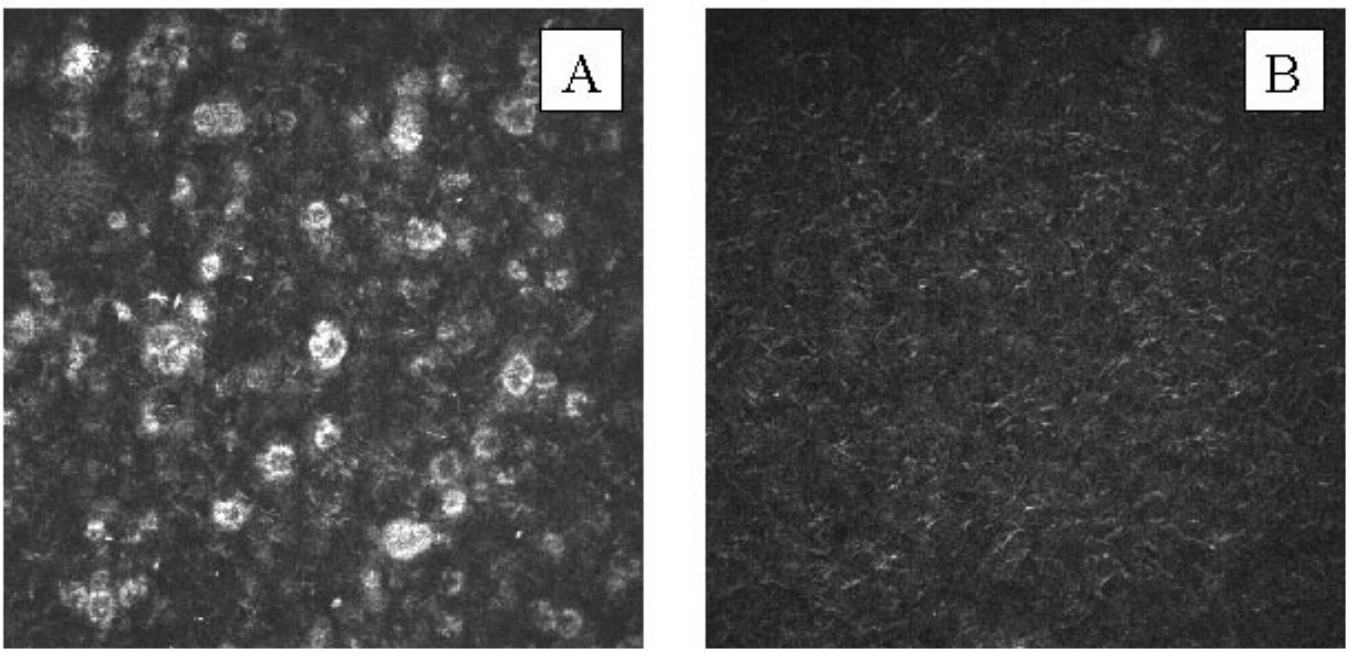

FIG. 1. Three-photon excitation fluorescence micrographs of anhydrous milk fat (AMF) (A) and milk fat triacylglycerols (MF-TAG) (B) crystallized at 20°C for 24 h under a coverslip.

TABLE 3
Fatty Acid Composition of Anhydrous Milk Fat (AMF) and MF-TAG[a]

Fatty acid	AMF (mol%)	MF-TAG (mol%)
4:0	10.37 ± 0.61	9.36 ± 0.97
6:0	5.41 ± 0.07	4.85 ± 0.08
8:0	2.04 ± 0.03	1.91 ± 0.01
10:0	3.97 ± 0.04	3.86 ± 0.10
12:0	4.04 ± 0.04	4.05 ± 0.16
14:0	11.00 ± 0.15	11.35 ± 0.36
14:1	1.83 ± 0.00	2.00 ± 0.18
15:0	1.19 ± 0.01	1.35 ± 0.16
16:0	26.12 ± 0.35	26.48 ± 0.02
16:1	2.56 ± 0.02	2.69 ± 0.14
17:0	0.66 ± 0.02	0.72 ± 0.07
18:0	8.59 ± 0.02	8.57 ± 0.09
18:1	19.26 ± 0.18	19.75 ± 0.28
18:2	2.41 ± 0.04	2.49 ± 0.05
18:3 and 18:2	0.58 ± 0.05	0.57 ± 0.02

[a]Determined by gas–liquid chromatography. Data reported represent the average of two replicates ± standard deviation. See Table 2 for abbreviation.

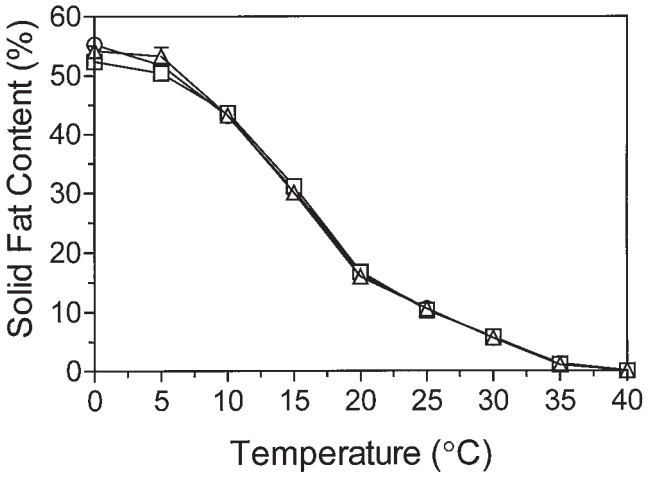

FIG. 2. Solid fat content (%) vs. temperature (°C) for anhydrous milk fat (AMF) (△), milk fat triacylglycerols (MF-TAG) (□), and MF-TAG with 0.1% diacylglycerols added back (MF-DAG) (○). Symbols represent the average ± standard error of three replicates.

crystallization, but this effect depended on the degree of supercooling. At high degrees of supercooling AMF, MF-TAG, and MF-DAG displayed identical crystallization profiles. All three fats crystallized very rapidly and reached the same SFC at 5.0, 10.0, and 15.0°C (Fig. 3). Similarly, King (1) found that minor lipids did not influence the crystallization patterns of rapidly cooled milk fat. At higher temperatures, the crystallization curves became more sigmoidal, and the effects of the minor components became more apparent. Between 20.0 and 27.5°C, AMF and MF-TAG exhibited different crystallization behaviors. MF-TAG started crystallizing earlier than AMF (Fig. 4). Addition of diacylglycerols to the MF-TAG shifted the crystallization behavior more closely to that of AMF. At 25.0 and 27.5°C crystallization in the MF-DAG was particularly delayed. At lower degrees of supercooling the minor components had an inhibitory effect on the crystallization process. Although they did not change the final amount of solid fat attained, minor components increased the induction time (Table 5). Induction times determined by turbidity measurements ($\tau_{turbidity}$) are also shown, and will be discussed later. Between 5.0 and 20.0°C, the induction times for AMF, MF-TAG, and MF-DAG were not significantly different ($P > 0.05$). However, at higher temperatures MF-TAG started crystallizing earlier than AMF, and MF-DAG had the longest induction times ($P < 0.001$).

TABLE 4
Triacylglycerol Composition of AMF and MF-TAG[a]

Triacylglycerol (carbon number)	AMF (wt%)	MF-TAG (wt%)
24	0.29 ± 0.00	0.21 ± 0.01
26	0.19 ± 0.01	0.15 ± 0.00
28	0.42 ± 0.02	0.36 ± 0.00
30	1.13 ± 0.07	0.86 ± 0.04
32	2.32 ± 0.00	2.26 ± 0.05
34	5.76 ± 0.07	5.98 ± 0.08
36	12.77 ± 0.16	13.35 ± 0.08
38	14.53 ± 0.10	15.32 ± 0.11
40	11.78 ± 0.14	12.34 ± 0.01
42	8.27 ± 0.03	8.70 ± 0.04
44	7.58 ± 0.00	7.76 ± 0.04
46	8.26 ± 0.03	8.15 ± 0.03
48	9.37 ± 0.08	8.99 ± 0.00
50	9.65 ± 0.13	8.54 ± 0.00
52	7.91 ± 0.37	6.69 ± 0.00

[a]Average of two replicates and standard deviation. For abbreviations see Table 2 and 3.

To quantify differences in the crystallization behaviors of AMF, MF-TAG, and MF-DAG, the SFC crystallization curves were fitted to the Avrami equation by nonlinear regression. The equation fitted the data very well over the entire range of fractional crystallization; correlation coefficients were always greater than 0.96. The Avrami rate constants (k), half times of crystallization ($t_{1/2}$), and exponents (n) are shown in Table 6.

Avrami constants (k) decreased as the temperature increased. The largest drop in k occurred between 20.0 and 22.5°C. Here, over only a couple of degrees, the Avrami constants drop by a factor of roughly 1000. Over the entire 5.0 to 20.0°C range, k for AMF, MF-TAG, and MF-DAG only decreased by a factor of 10. Up to 20.0°C, temperature had a very strong influence on k ($P < 0.001$). Between 22.5 and 27.5°C, there was no significant effect of temperature on the Avrami constant ($P > 0.05$). No significant differences were observed between k for AMF and the MF-TAG ($P > 0.05$), although the MF-DAG had significantly lower Avrami constants ($P < 0.001$). The native mixture of minor components does not seem to affect the rate of milk fat crystallization. Diacylglycerols alone, however, seem to slow the rate. The increase in $t_{1/2}$ for all three fats as a function of increasing temperature reflects the decrease in k at higher temperatures.

Changes in the Avrami constant as a function of crystallization temperature are shown in Figure 5. These graphs demonstrate the existence of two distinct regions, one above

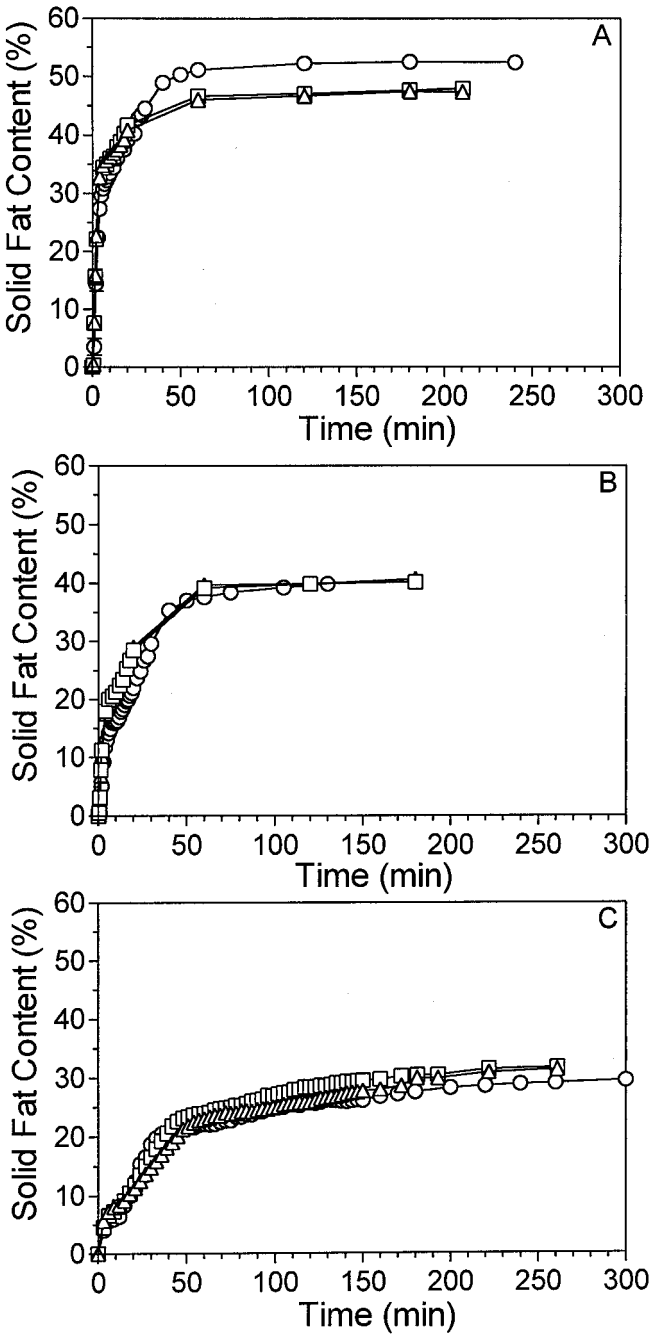

FIG. 3. Solid fat content (%) vs. time during static crystallization of AMF (△), MF-TAG (□), and MF-DAG (○) at 5.0 (A), 10.0 (B), and 15.0°C (C). Symbols represent the average ± standard error of three replicates. For abbreviations see Figure 2.

and the other below 20.0°C. The division between these two regions is very pronounced. Figure 5B shows that the Avrami exponent remains constant and low (around 0.60) when the temperature is low. Here, between 5.0 and 15.0°C, temperature had no significant effect on n ($P > 0.05$). This is not surprising since n generally tends to remain constant over an appreciable temperature range and is independent of the degree of supercooling (34,36). Around 20°C, n began to increase. This is the same point at which the greatest change in the Avrami constant occurred. Above 20.0°C, n continued to increase as temperature was increased. Both above and below 20.0°C, no significant differences were observed between n for AMF and the MF-TAG ($P > 0.05$). Above 20°C, exponents for the MF-DAG were slightly higher than for both AMF and MF-TAG ($P < 0.001$), which reflects the more sigmoidal nature of the MF-DAG crystallization curves.

The similarities in Avrami exponents for AMF and the MF-TAG suggest that these fats crystallize in a similar fashion. The differences observed for MF-DAG may be indicative of slightly different modes of crystal growth owing to the presence of diacylglycerols. In AMF, MF-TAG, and MF-DAG, the sharp change in n around 20.0°C suggests the existence of different crystallization mechanisms depending on the degree of supercooling. The change in n at about this point should indicate differences in crystal growth geometry (34). Milk fat crystallizes predominantly in the β′-crystal form, although at high rates of cooling (≥1°C/min) the α crystal will form below 20.0°C. The α crystal is a metastable form and has a clear point of 20.0°C when the triacylglycerols transform to the more stable β′-crystal (43). The sharp change observed in the crystallization mode around 20.0°C is perhaps related to the formation of the α-crystal at the lower temperatures.

An increase in the induction time and a more sigmoidal crystallization curve are generally indicated by a higher Avrami exponent (27,37). This was found to be true; at higher temperatures, values of τ and n were significantly higher, and crystallization curves appeared more sigmoidal. According to Sharples (37), below 20°C the experimental n of roughly 0.6 may suggest rod-like growth in only one dimension from instantaneous nuclei. Generally, as the rate of crystallization increases the growth mechanism changes from lineal to polyhedral, as indicated by an increase in the Avrami exponent (27). The experimental increase in n suggests that crystal growth above 20.0°C changes from a one- to a multidimensional event.

Beyond this it is impossible to draw unambiguous conclusions about the growth mechanism based on the determined Avrami exponent, unless the type of growth can be verified microscopically. The situation is further complicated by the fact that, although n should be an integer, fractional values are obtained in some analyses, even in cases where the Avrami equation is very accurately obeyed (37). Fractional values for n were consistently obtained from the AMF, MF-TAG, and MF-DAG crystallization curves, despite correlation coefficients of at least 0.96. Christian (34) reported that for some cases of metals and alloys in which growth is diffusion controlled, fractional exponents correlate with specific growth mechanisms. In such cases an exponent of roughly 0.5 may indicate precipitation on crystal dislocations. Similarly, values greater than 2.5 reflect growth of all shapes with increasing nucleation rate (34).

Although the Avrami equation is being used increasingly in fat research, it has limitations when the nature of the growth process cannot be visualized. The resolution of crystal nuclei and the initial stages of growth are beyond the ca-

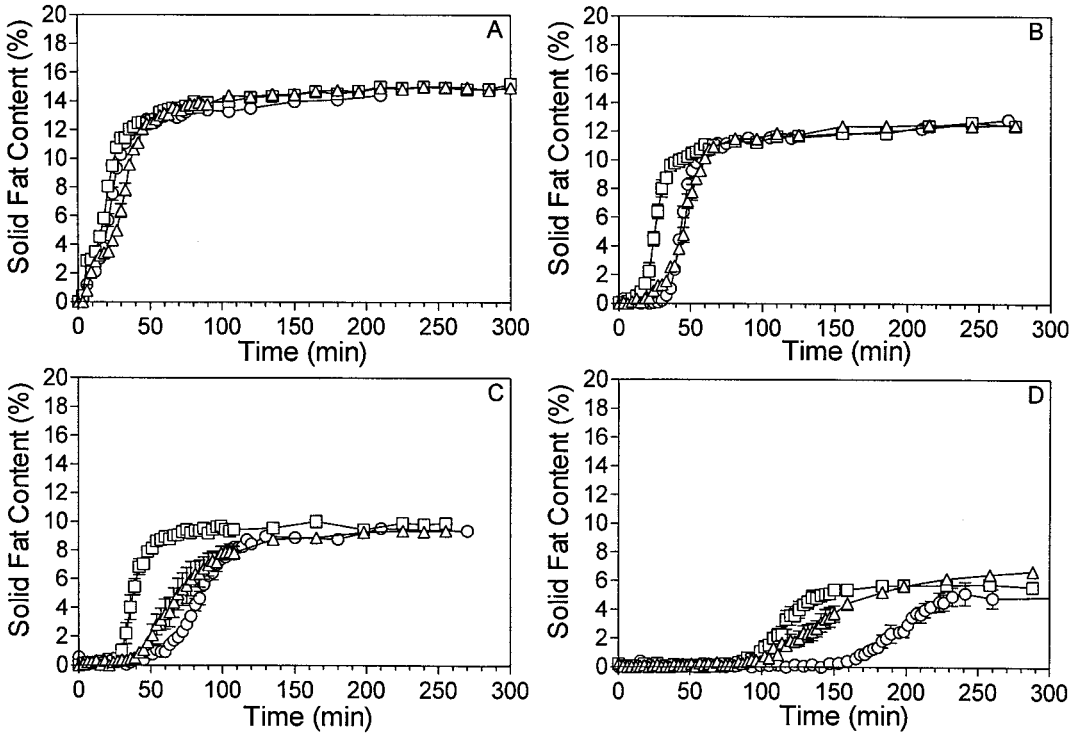

FIG. 4. Solid fat content (%) vs. time during static crystallization of AMF (△), MF-TAG (□), and MF-DAG (○) at 20.0 (A), 22.5 (B), 25.0 (C), and 27.5°C (D). Symbols represent the average ± standard error of three replicates. For abbreviations see Figure 2.

pabilities of a light microscope, so it is impossible to make definite conclusions about the modes of crystal growth observed at different temperatures. Having said this, the Avrami exponent does provide a phenomenological index of crystallization. Accordingly, the similarities in *n* between AMF and MF-TAG point to the fact that removal of the minor components does not change the growth mode, and the distinct change in the exponent around 20°C suggests a change in crystal growth mechanism in both fats around this temperature.

Increases in turbidity of AMF, MF-TAG, and MF-DAG during crystallization at 15.0, 20.0, 22.5, 25.0, and 27.5°C are shown in Figure 6. Induction times derived from these plots ($\tau_{turbidity}$) are shown in Table 5. At 15.0 and 20.0°C no differences were observed between AMF and the MF-TAG (Fig. 6). Above 20.0°C, however, significant differences were observed in $\tau_{turbidity}$. MF-TAG consistently had shorter induction times than AMF ($P < 0.001$). These trends were similar to those when monitoring crystallization using pNMR; absence of minor components in MF-TAG resulted in an earlier onset of crystallization. The situation with the diacylglycerols is more complicated. At 15.0 and 20.0°C $\tau_{turbidity}$ for MF-DAG was not significantly different from that of AMF and MF-TAG ($P > 0.05$), while above that MF-DAG had the shortest induction time ($P < 0.001$) (Table 5). Each MF-DAG turbidity curve had an initial rise very early in the process,

TABLE 5
Induction Times (min) for Crystallization of AMF, MF-TAG, and MF-DAG[a]

Temperature (°C)	Induction time by SFC (τ_{SFC})			Induction time by turbidity ($\tau_{turbidity}$)		
	AMF	MF-TAG	MF-DAG	AMF	MF-TAG	MF-DAG
5.0	0.05 ± 0.00^{K}	0.05 ± 0.00^{K}	0.05 ± 0.00^{K}	ND	ND	ND
10.0	0.50 ± 0.00^{K}	0.50 ± 0.00^{K}	0.50 ± 0.00^{K}	ND	ND	ND
15.0	2.00 ± 0.00^{K}	1.83 ± 0.17^{K}	2.00 ± 0.00^{K}	6.78 ± 0.11^{F}	6.89 ± 0.11^{F}	6.11 ± 0.45^{F}
20.0	5.33 ± 0.33^{J}	4.33 ± 0.33^{J}	5.33 ± 0.33^{J}	$8.33 \pm 0.58^{E,F}$	7.22 ± 0.29^{F}	$8.11 \pm 0.29^{E,F}$
22.5	23.33 ± 0.67^{H}	14.83 ± 0.17^{I}	35.33 ± 0.33^{F}	$12.67 \pm 1.02^{D,E,}$	$9.11 \pm 0.29^{E,F}$	$10.00 \pm 0.84^{D,E,F}$
25.0	45.33 ± 0.17^{E}	29.83 ± 0.17^{G}	57.00 ± 0.58^{D}	23.22 ± 2.35^{C}	14.56 ± 0.48^{D}	$12.11 \pm 0.59^{D,E}$
27.5	107.83 ± 0.17^{B}	95.67 ± 0.17^{C}	163.67 ± 0.88^{A}	40.22 ± 1.47^{A}	31.00 ± 0.67^{B}	20.78 ± 1.50^{C}

[a]Determined by SFC (τ_{SFC}) and turbidity measurements ($\tau_{turbidity}$) at 5.0, 10.0, 15.0, 20.0, 22.5, 25.0, and 27.5°C. Mean value of three replicates ± standard error of the mean. Different superscript letters (A–K) indicate significant differences ($P < 0.05$) in each column. Comparisons were made between AMF, MF-TAG, and MF-DAG within τ_{SFC} and separately within $\tau_{turbidity}$. MF-DAG, milk fat triacylglycerols with diacylglycerols added back; SFC, solid fat content; ND, not determined; for other abbreviations see Table 2.

TABLE 6
Avrami Constant, *k*, Half Times of Crystallization $t_{1/2}$, and Avrami Exponents *n* of AMF, MF-TAG, and MF-DAG Crystallized at 5.0, 10.0, 15.0, 20.0, 22.5, 25.0, and 27.5°C[a]

Temperature (°C)	*k* (t^{-k})	$t_{1/2}$ (min)	*n*
AMF			
5.0	$3.1 \times 10^{-1} \pm 0.2 \times 10^{-1A}$	3.47 ± 0.20^{K}	0.65 ± 0.01^{F}
10.0	$1.7 \times 10^{-1} \pm 0.4 \times 10^{-1B}$	10.28 ± 1.69^{K}	0.61 ± 0.03^{F}
15.0	$6.9 \times 10^{-2} \pm 0.2 \times 10^{-2C}$	36.26 ± 0.75^{K}	0.64 ± 0.00^{F}
20.0	$4.0 \times 10^{-3} \pm 1.0 \times 10^{-3D}$	32.33 ± 3.46^{J}	1.52 ± 0.04^{E}
22.5	$1.6 \times 10^{-7} \pm 0.5 \times 10^{-7D}$	61.36 ± 14.65^{H}	3.96 ± 0.03^{C}
25.0	$2.5 \times 10^{-6} \pm 2.5 \times 10^{-6D}$	74.11 ± 12.21^{E}	3.01 ± 0.16^{D}
27.5	$6.6 \times 10^{-10} \pm 8.2 \times 10^{-10D}$	165.65 ± 51.28^{B}	$4.35 \pm 0.22^{B,C}$
MF–TAG			
5.0	$3.0 \times 10^{-1} \pm 0.3 \times 10^{-1A}$	3.59 ± 0.32^{K}	0.66 ± 0.02^{F}
10.0	$1.6 \times 10^{-1} \pm 0.1 \times 10^{-1B}$	10.08 ± 0.59^{K}	0.65 ± 0.01^{F}
15.0	$6.0 \times 10^{-2} \pm 1.0 \times 10^{-2C}$	33.55 ± 4.07^{K}	0.69 ± 0.02^{F}
20.0	$9.0 \times 10^{-2} \pm 0.0 \times 10^{-2C}$	23.93 ± 0.86^{J}	0.66 ± 0.01^{F}
22.5	$2.3 \times 10^{-5} \pm 4.4 \times 10^{-5D}$	27.45 ± 1.36^{I}	2.41 ± 0.05^{F}
25.0	$1.6 \times 10^{-7} \pm 1.2 \times 10^{-7D}$	54.54 ± 9.23^{G}	$3.93 \pm 0.18^{B,C}$
27.5	$3.0 \times 10^{-11} \pm 2.5 \times 10^{-11D}$	126.92 ± 11.31^{C}	$4.98 \pm 0.06^{A,B}$
MF–DAG			
5.0	$2.7 \times 10^{-1} \pm 0.4 \times 10^{-1A}$	5.26 ± 0.64^{K}	0.59 ± 0.00^{F}
10.0	$8.5 \times 10^{-2} \pm 0.3 \times 10^{-2A}$	16.53 ± 0.42^{K}	$0.75 \pm 0.00^{E,F}$
15.0	$8.3 \times 10^{-2} \pm 0.1 \times 10^{-2A}$	27.91 ± 0.43^{K}	0.64 ± 0.01^{F}
20.0	$1.0 \times 10^{-2} \pm 0.4 \times 10^{-2C}$	25.81 ± 3.93^{J}	$1.33 \pm 0.06^{E,F}$
22.5	$2.4 \times 10^{-8} \pm 2.7 \times 10^{-8D}$	49.8 ± 13.19^{F}	$4.69 \pm 0.32^{A,B,C}$
25.0	$2.6 \times 10^{-9} \pm 1.8 \times 10^{-9D}$	87.22 ± 15.92^{D}	$4.52 \pm 0.18^{B,C}$
27.5	$4.9 \times 10^{-12} \pm 8.5 \times 10^{-12D}$	234.90 ± 80.08^{A}	5.46 ± 0.43^{A}

[a]Mean value of three replicates ± standard error of the mean. Different superscript letters (A–K) indicate significant differences ($P < 0.05$) within either *k*, $t_{1/2}$, or *n* columns. For abbreviations see Tables 3 and 5.

but this bump leveled off until $\tau_{turbidity}$ was surpassed. Possibly the presence of the diacylglycerols led to an increase in crystal mass very early on. Nuclei may have been formed initially, encouraged by the diacylglycerol presence, but did not develop appreciably for some time until $\tau_{turbidity}$ was exceeded.

The Fisher-Turnbull equation can be used to calculate activation free energies of nucleation based on experimentally determined induction times of nucleation (44). Strictly speaking, this practice is valid only if the induction times relate exclusively to nucleation and do not include crystal growth as well. In fat crystallization studies it has become popular to use induction times determined by turbidimetric methods ($\tau_{turbidity}$) for the purpose. Because the Fisher-Turnbull equation may be useful for comparing crystallization events between fats and with previous studies, we have calculated the activation free energies of nucleation (ΔG_c). However, because there is no assurance that the turbidity induction times only represent nucleation, we will consider the calculated free energies to be apparent activation free energies of nucleation ($\Delta G_{c,apparent}$). $\Delta G_{c,apparent}$ values were not calculated from SFC induction times, because these are clearly not induction times of nucleation. Tiny crystals are sometimes visible in the melt before the pNMR signal detects the presence of crystal mass.

As expected, temperature had a significant effect on $\Delta G_{c,apparent}$ ($P < 0.001$). $\Delta G_{c,apparent}$ increased with increasing temperature (Table 7). AMF, MF-TAG, and MF-DAG had significantly different $\Delta G_{c,apparent}$ ($P < 0.001$), suggesting that milk fat minor components had an effect on the energy barrier to nucleation. The higher $\Delta G_{c,apparent}$ for AMF over the MF-TAG suggests that nucleation in AMF occurs less readily than in the MF-TAG. Lower induction times translate into lower $\Delta G_{c,apparent}$. MF-DAG consistently had lower $\Delta G_{c,apparent}$ than AMF and MF-TAG ($P < 0.001$), which might indicate a lower energy barrier to nucleation in the MF-DAG as suggested by the lower induction times (Table 5) and turbidity profiles during crystallization (Fig. 6).

Previously, good agreement was found between increases in crystal mass and turbidity during crystallization (45,46). Figure 7 shows good agreement between the $\tau_{turbidity}$ and τ_{SFC} for AMF, MF-TAG, and MF-DAG. This supports the fact that increases in turbidity are due to mass deposition and not just to nucleation, and lends support to considering nucleation free energies, calculated based on the Fisher-Turnbull equation, as apparent free energies. Nucleation and crystal growth are not necessarily distinct events but can occur simultaneously (47). Initial increases in turbidity during crystallization may reflect only nucleation in cases where all nucleation occurs very early on and quite independently from crystal growth. However, in cases of sporadic nucleation, where more nuclei appear in time, as other nuclei grow, $\tau_{turbidity}$ is not a nucleation induction time. The good agreement between increases in turbidity and SFC during crystallization means

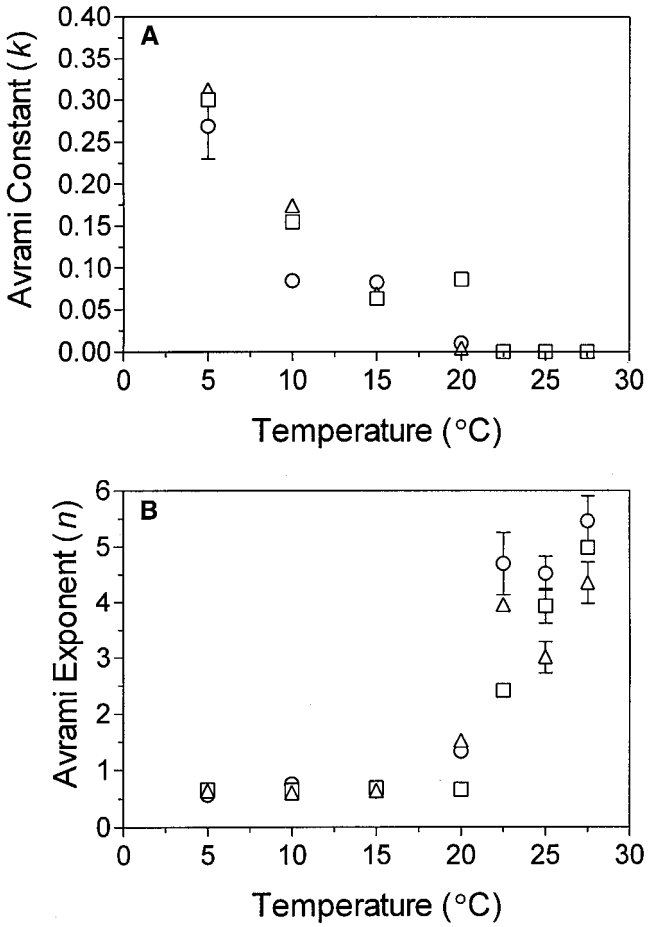

FIG. 5. Avrami rate constants *k* (A) and exponents *n* (B) for AMF (△), MF-TAG (□), and MF-DAG (○) as a function of crystallization temperature. Symbols represent the average ± standard error of three replicates. For abbreviations see Figure 2.

that turbidity may reasonably replace pNMR or crystal mass measurements to monitor on-line crystallization processes. However, according to SFC measurements MF-DAG consistently crystallized later than AMF and MF-TAG, whereas by turbidity measurements MF-DAG crystallized before the other fats at 25.0 and 27.5°C (Table 5). This discrepancy in the trends observed by both methods means that the pNMR and spectrographic methods are not entirely equivalent.

The positional distribution of fatty acids in milk fat diacylglycerols is compared with that of milk fat in Table 8. The diacylglycerols are enriched in palmitic acid at the *sn*-1,3 position. This may encourage interactions with the milk fat triacylglycerols which contain more palmitic acid at the *sn*-2 position, allowing the diacylglycerols to cocrystallize with the triacylglycerols. Possibly the milk fat diacylglycerols encourage nucleation (bump in turbidity profiles in Fig. 6); however, overall they exert an inhibitory effect on crystal growth. Figure 8 shows that when 0.1 wt% dipalmitin (mixed isomers) was added back to the MF-TAG, crystallization at 22.5°C began earlier. Dipalmitin is a high-melting compound that likely acts as a seed, crystallizing out before the MF-TAG and subsequently inducing nucleation and crystal growth. Dipalmitin and the milk fat diacylglycerols have different rates of crystallization and therefore interact differently with the MF-TAG. Complementarity between the milk fat diacylglycerols and triacylglycerols may allow the diacylglycerols to cocrystallize with the MF-TAG and be incorporated into the embryos or growing crystals. Upon incorporation they seem to retard crystallization. Dipalmitin, on the other hand, enhances crystallization.

Figure 9 shows polarized light micrographs of AMF, MF-TAG, and MF-DAG after crystallization for 5 d at 5.0 and 25.0°C. No differences were observed between the three fats at either temperature. Removal of the minor components did not affect the formation of the typical crystal microstructure of AMF. The influence of temperature on crystal network structure, however, is very obvious. With a high degree of supercooling (roughly 28° at 5.0°C), nucleation proceeds very rapidly, and the resulting pattern of crystal structures resembles a starry night. At higher temperatures (25.0°C), there is more time for the crystals to arrange into more ordered microstructures.

X-ray diffraction (XRD) patterns of AMF, MF-TAG, and MF-DAG at 5 and 25°C were identical. The patterns for AMF, MF-TAG and MF-DAG at 5°C are shown in Figure 10. Reflections at 3.8, 4.2, and 39 Å were detected in all three fats

TABLE 7
Apparent Activation Free Energies of Nucleation ($\Delta G_{c,apparent}$) for AMF, MF-TAG, and MF-DAG Crystallized at 15.0, 20.0, 22.5, 25.0, and 27.5°C[a]

Temperature (°C)	AMF (kJ/mol)	MF-TAG (kJ/mol)	MF-DAG (kJ/mol)
15.0	$0.61 \pm 0.01^{H,J}$	$0.54 \pm 0.01^{I,J}$	0.36 ± 0.03^{J}
20.0	$1.12 \pm 0.03^{F,G}$	$0.99 \pm 0.02^{G,H,I}$	$0.67 \pm 0.05^{H,I,J}$
22.5	1.66 ± 0.04^{E}	$1.47 \pm 0.03^{E,F}$	$0.99 \pm 0.07^{G,H}$
25.0	2.46 ± 0.06^{D}	2.18 ± 0.05^{D}	$1.48 \pm 0.11^{E,F}$
27.5	5.18 ± 0.13^{A}	4.59 ± 0.10^{B}	3.11 ± 0.23^{C}

[a]Mean value of three replicates ± standard error of the mean. Different superscript letters (A–J) indicate significant differences ($P < 0.05$) between values. For abbreviations see Tables 3 and 5.

TABLE 8
Fatty Acid Positional Distribution (mol%) of AMF[a] and Milk Fat Diacylglycerols

	AMF		Diacylglycerols	
Fatty acid	*sn*-2	*sn*-1,3	*sn*-2	*sn*-1,3
4:0	0.0	18.4	0.0	0.0
6:0	0.0	4.2	4.1	0.2
8:0	0.0	2.2	2.3	0.1
10:0	4.1	3.9	3.8	1.4
12:0	8.3	3.5	4.8	3.5
14:0	19.2	18.8	11.9	13.6
16:0	35.7	20.4	21.9	43.7
18:0	11.5	9.4	7.5	12.2
18:1	21.0	19.3	9.0	16.0

[a]After Willis and Marangoni (48). For abbreviation see Table 3.

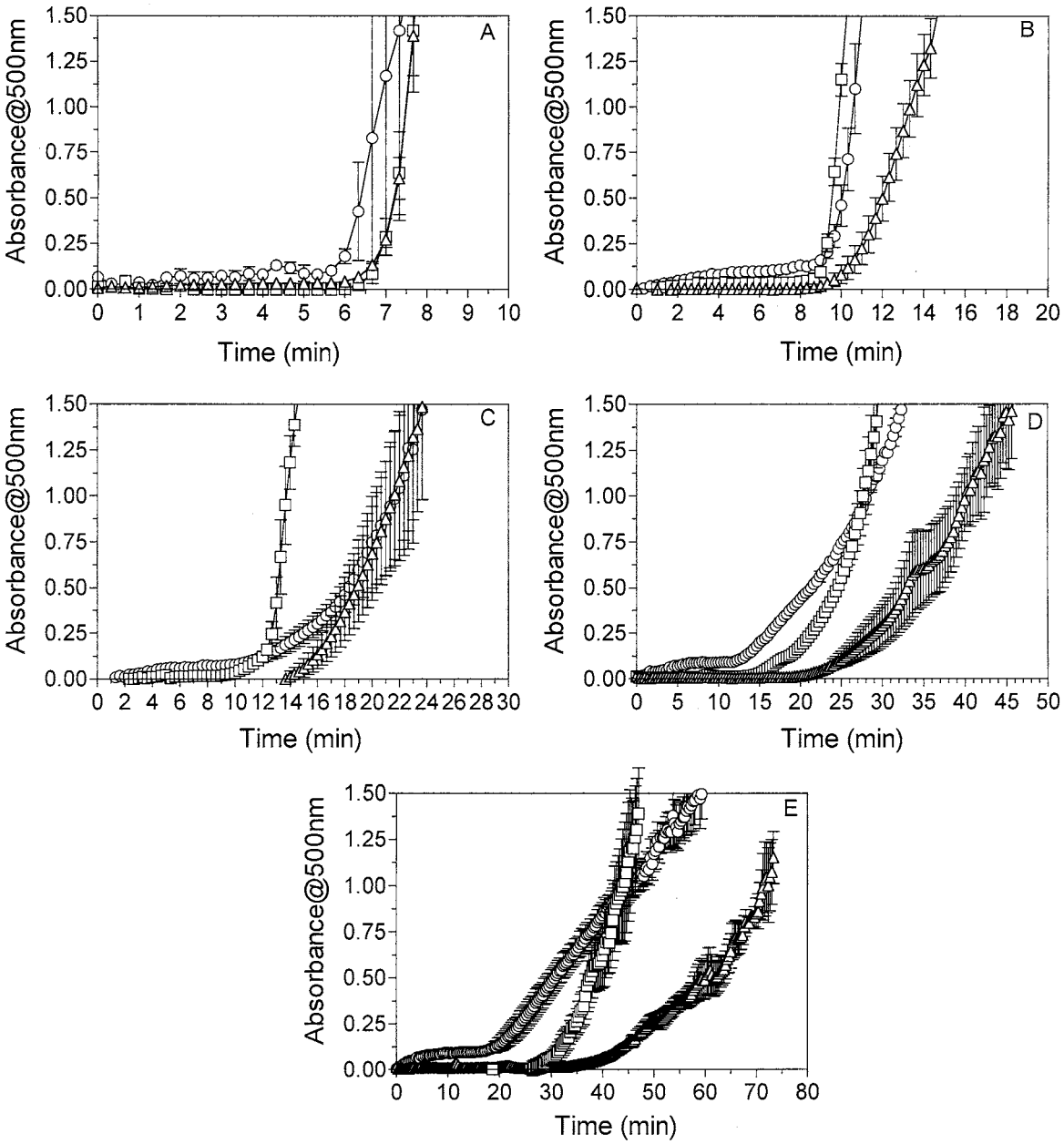

FIG. 6. Increase in absorbance measured at 500 nm with time during crystallization of AMF (△), MF-TAG (□), and MF-DAG (○) at 15.0 (A), 20.0 (B), 22.5 (C), 25.0 (D), and 27.5°C (E). Symbols represent the average ± standard error of three replicates. For abbreviations see Figure 2.

at both temperatures. The reflections nearest the center of each image represent the long spacings, whereas the outer two reflection rings are the short spacings. The XRD patterns indicate that the absence of minor components and presence of only milk fat diacylglycerols did not alter the formation of milk fat's typical β′-2 polymorphic form. In Figure 11 τ_{SFC} and $\tau_{turbidity}$ are plotted as a function of temperature. This type of plot indicates whether different polymorphic forms are present in the temperature range studied. A continuous curve indicates that at all temperatures the same crystal polymorph is formed, while a discontinuous curve indicates the existence of different polymorphs (31,44,48). The discontinuity of the curves in Figure 11 suggests that AMF, the MF-TAG, and the MF-DAG may crystallize in a different polymorphic form above and below 20.0°C. The discontinuity is especially obvious in the plot with induction times by SFC (indicated by arrow in Fig. 11B). This evidence supports the hypothesis that different crystallization modes above and below 20.0°C, as indicated by the Avrami parameters (Fig. 5), are related to formation of the α-crystal below this temperature (43). The clear point of the α-crystal is approximately 20°C (43). Below 20°C, α-crystals form more readily, and therefore there is an increased number of nuclei present. Above 20°C, however, there are fewer nuclei formed and crystal growth predominates. The isothermal DSC crystallization and melting curves for AMF, MF-TAG, and MF-DAG are shown in

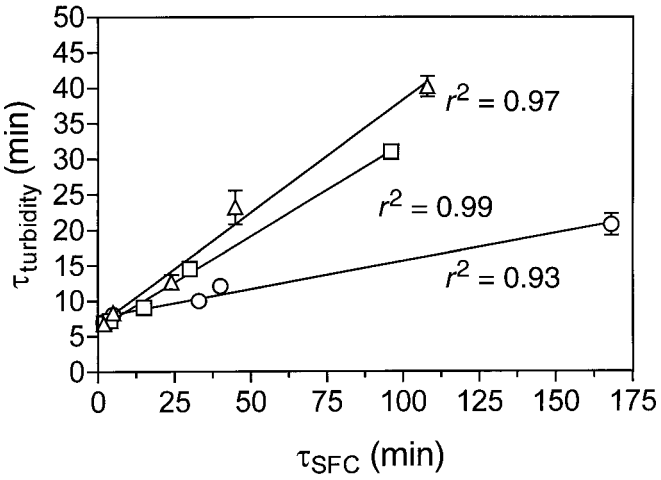

FIG. 7. Induction time by turbidity ($\tau_{turbidity}$) vs. induction time by SFC (τ_{SFC}) for AMF (△), MF-TAG (□), and MF-DAG (○) crystallized at 5.0, 10.0, 15.0, 20.0, 22.5, 25.0, and 27.5°C. For abbreviations see Figure 2.

Figure 12. No differences are observed between the three samples. Consistently the onset crystallization temperature was roughly 18°C, and the peak melting temperature was around 20°C.

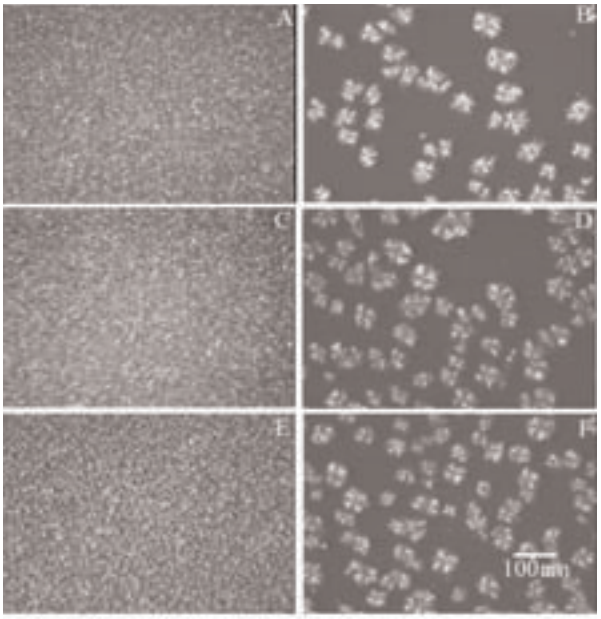

FIG. 9. Polarized light micrographs of AMF, MF-TAG, and MF-DAG (○) crystallized at 5.0 and 25.0°C. (A) AMF crystallized at 5.0%C; (B) AMF crystallized at 25.0°C; (C) MF-TAG crystallized at 5.0°C; (D) MF-TAG crystallized at 25.0°C; (E) MF-DAG crystallized at 5.0°C; (F) MF-DAG crystallized at 25.0°C. For abbreviations see Figure 2.

ACKNOWLEDGMENTS

The authors acknowledge the financial assistance of the Natural Sciences and Engineering Research Council of Canada (NSERC), Dr. Michael Jennings of the University of Western Ontario for his assistance with the XRD analysis, and Frank Mena of the University of Guelph for his assistance with the GC–MS analysis.

REFERENCES

1. King, N., The Effect of Some Surface Active Substances on the Physical Forms of Milk Fat, *Proceedings of the 17th International Dairy Congress*, Munich, 1966, *C*:2, pp. 289–294.
2. Morrison, W.R., Surface-Active Lipids in Milk and Milk Products, in *Surface-Active Lipids in Foods*, S.C.I. Monograph No. 32, Society of Chemical Industry, London, 1968, pp. 75–91.
3. Kapsalis, J.G., J.J. Betscher, T. Kristoffersen, and I.A. Gould, Effect of Chemical Additives on the Spreading Quality of Butter. I. The Consistency of Butter as Determined by Mechanical and Consumer Panel Evaluation Methods, *J. Dairy Sci. 43*: 1560–1564 (1960).
4. Kapsalis, J.G., T. Kristoffersen, I.A. Gould and J.J. Betscher, Effect of Chemical Additives on the Spreading Quality of Butter. II. Laboratory and Plant Churnings, *Ibid. 46*:107–113 (1963).
5. DuRoss, J.W., and W.H. Knightly, Relationship of Sorbitan Monostearate and Polysorbate 60 to Bloom Resistance in Properly Tempered Chocolate, *Manuf. Confect. July*:50–56 (1965).
6. van den Tempel, M., Effects of Emulsifiers on the Crystallization of Triglycerides, in *Surface-Active Lipids in Foods*, S.C.I. Monograph No. 32, Society of Chemical Industry, London, 1968, pp. 22–33.
7. Aronhime, J., S. Sarig, and N. Garti, Emulsifiers as Additives in Fats: Effect on Polymorphic Transformations and Crystal Properties of Fatty Acids and Triglycerides, *Food Structure 9*: 337–352 (1990).
8. Hernqvist, L., and K. Anjou, Diglycerides as a Stabilizer of the Beta Prime Crystal Form in Margarines and Fats, *Fette Seifen Anstrichm. 85*(2):64–66 (1983).
9. Loncin, M., Influence des glycerides partiels sur la plasticite des matières grasses, *Oleagineux 13*:33–37 (1958).
10. Siew, W.L., and W.L. Ng, Effect of Diglycerides on the Crystallisation of Palm Oleins, *J. Sci. Food Agric. 71*:496–500 (1996).
11. Gordon, M.H., and I.A. Rahman, Effects of Minor Components on the Crystallization of Coconut Oil, *J. Am. Oil Chem. Soc. 68*: 577–579 (1991).
12. Cebula, D., and K. Smith, Differential Scanning Calorimetry of Confectionary Fats: Part II. Effects of Blends and Minor Components, *J. Am. Oil Chem. Soc. 69*:992–998 (1992).

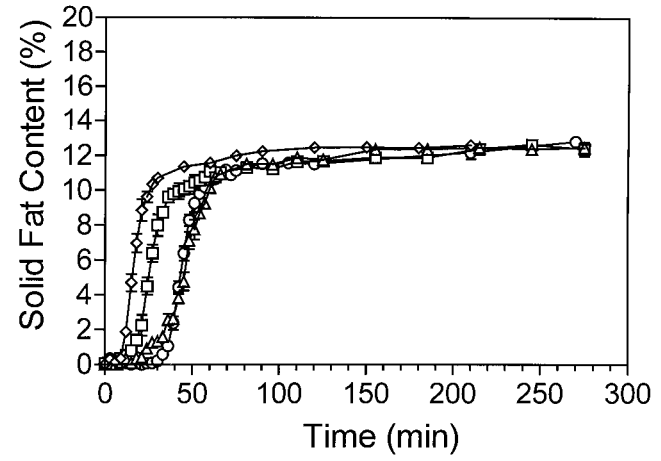

FIG. 8. Solid fat content (%) vs. time during static crystallization of AMF (△), MF-TAG (□), and MF-DAG (○), and MF-TAG with 0.1% dipalmitin (◇) at 22.5°C. Symbols represent the average ± standard error of three replicates. For abbreviations see Figure 2.

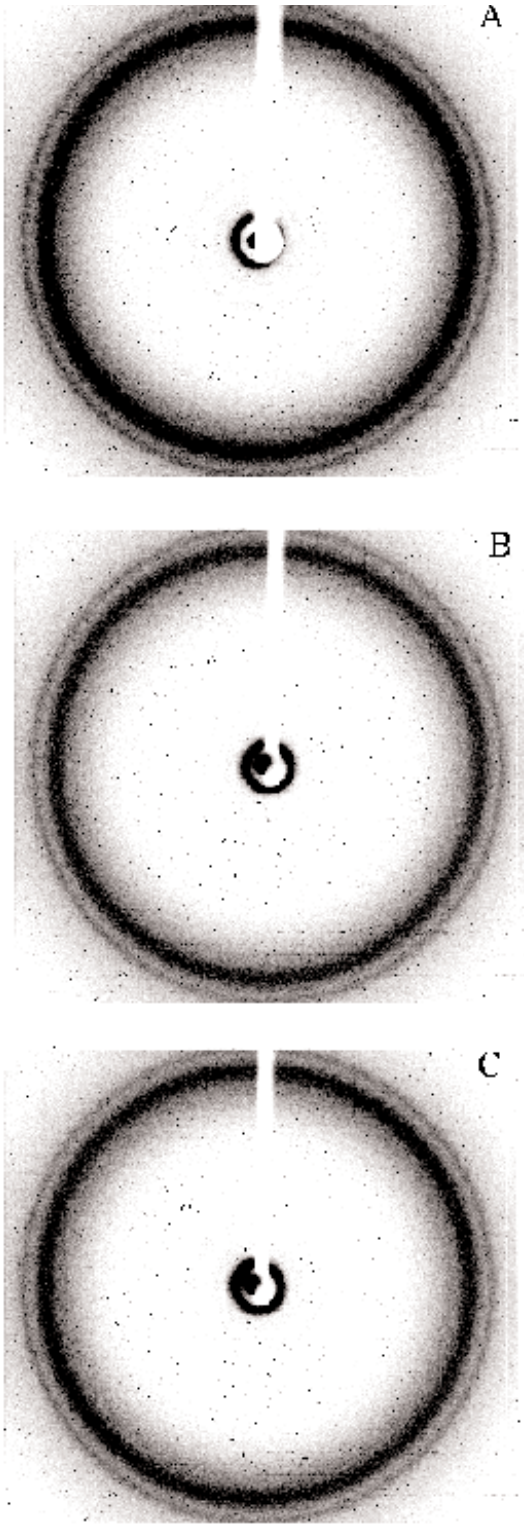

FIG. 10. Powder X-ray diffraction patterns of (A) AMF, (B) MF-TAG, and (C) MF-DAG at 5.0°C. For abbreviations see Figure 2.

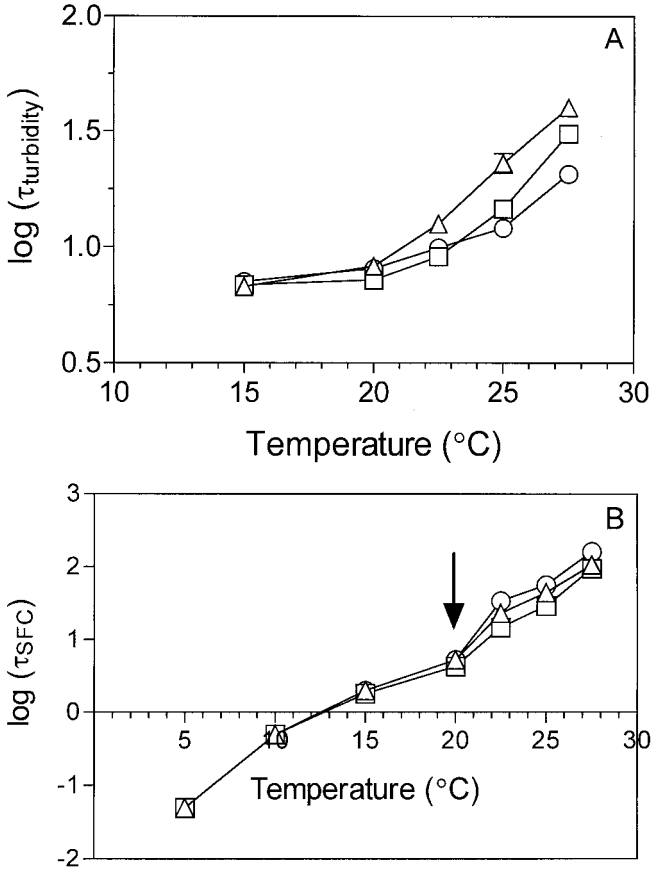

FIG. 11. Plot of log ($\tau_{turbidity}$) vs. crystallization temperature (A) and log (τ_{SFC}) vs. crystallization temperature (B). The discontinuity of the curves suggests the formation of different polymorphic forms upon crystallization above and below 20.0°C. AMF (△); MF-TAG (□); MF-DAG (○). For abbreviations see Figure 2.

13. Davis, T.R., and P.S. Dimick, Isolation and Thermal Characterization of High-Melting Seed Crystals Formed During Cocoa Butter Solidification, *Ibid*. *66*:1488–1493 (1989).
14. Davis, T.R., and P.S. Dimick, Lipid Composition of High-Melting Seed Crystals Formed During Cocoa Butter Solidification, *Ibid*. *66*:1494–1498 (1989).
15. Niiya, I., T. Maruyama, M. Imamura, M. Okada, and T. Matsumoto. Effect of Emulsifiers on the Crystal Growth of Edible Solid Fats. Part III. Effect of Saturated Fatty Acid Monoglyceride, *Jpn. J. Food Sci. Technol. 20*:182–189 (1973).
16. Niiya, I., T. Maruyama, M. Imamura, M. Okada, and T. Matsumoto, Effect of Emulsifiers on the Crystal Growth of Edible Solid Fats. Part IV. Effect of Propylene Glycol Ester of Fatty Acid and Unsaturated Fatty Acid Monoglycerides, *Ibid*. *20*: 191–198 (1973).
17. Reddy, S.Y., Effect of Diglycerides on the Solidification Properties of Sal *(Shorea robusta)* Fat, *Fat Sci. Technol. 10*: 394–397 (1987).
18. Riiner, U., The Effect of Hydrolysis on the Solidification of Fats. *Lebensm. Wiss. Technol*. *4*(3):76–80 (1971).
19. Gerson, T., and W.L. Escher, The Effect of Monoglycerides on the Spreadability of Butter, *N.Z.J. Sci*. *9*:528–533 (1966).
20. Carroll, K.K., Separation of Lipid Classes by Chromatography on Florisil, *J. Lipid Res. 2*:135–141 (1961).
21. Christie, W.W., *Lipid Analysis; Isolation, Separation, Identification, and Structural Analysis of Lipids*, 2nd edn., Pergamon Press, London, 1988, pp. 93–96, 115–119.
22. Bannon, C.D., J.D. Craske, and A.E. Hilliker, Analysis of Fatty Acid Methyl Esters with High Accuracy and Reliability. IV.

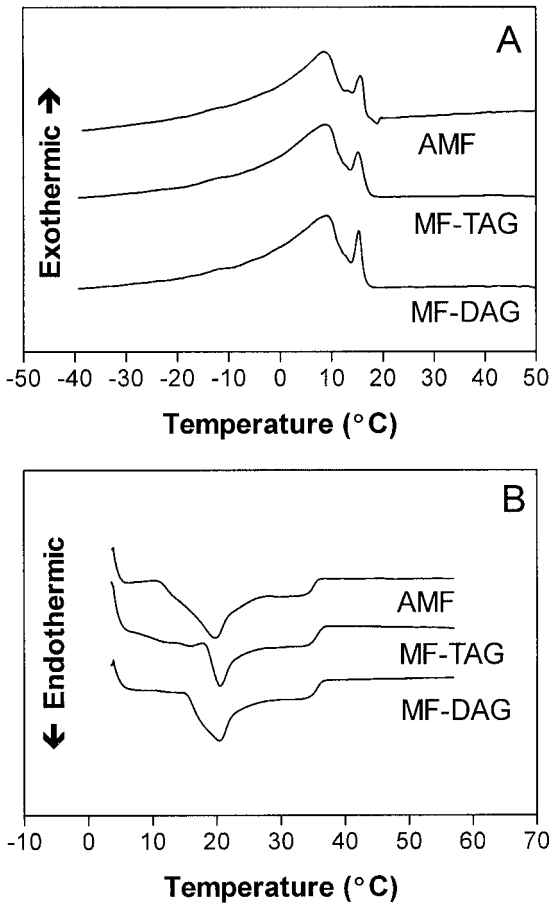

FIG. 12. Differential scanning calorimetric curves of AMF, MF-TAG, and MF-DAG in the crystallization (A) and melting (B) modes at 5.0°C/min. For abbreviations see Figure 2.

Fats with Fatty Acids Containing Four or More Carbon Atoms, *J. Am. Oil Chem. Soc*. *62*:1501–1507 (1985).
23. Rousseau, D., K. Forestiere, A.R. Hill, and A.G. Marangoni, Restructuring Butterfat Through Blending and Chemical Interesterification. 1. Melting Behavior and Triacylglycerol Modifications, *Ibid*. *73*:963–972 (1996).
24. *Official Methods and Recommended Practices of the American Oil Chemists' Society*, 4th edn., AOCS Press, Champaign, 1993.
25. Marangoni, A.G., On the Use and Misuse of the Avrami Equation in Characterization of the Kinetics of Fat Crystallization, *Ibid*. *75*:1465–1467 (1998).
26. Avrami, M., Kinetics of Phase Change I. General Theory, *J. Chem. Phys*. *7*:1103–1112 (1939).
27. Avrami, M., Kinetics of Phase Change II. Transformation-Time Relations for Random Distribution of Nuclei, *Ibid*. *8*:212–224 (1940).
28. Avrami, M., Kinetics of Phase Change III. Granulation, Phase Change, and Microstructure, *Ibid. 9*:177–184 (1941).
29. Ziegleder, G., DSC Thermal Analysis and Kinetics of Cocoa Butter Crystallization, *Fat Sci. Technol*. *92*:481–485 (1990).
30. Herrera, M.L., C. Falabella, M. Melgarejo, and M.C. Añon, Isothermal Crystallization of Hydrogenated Sunflower Oil: II. Growth and Solid Fat Content, *J. Am. Oil Chem. Soc*. *76*:1–6 (1998).
31. Dibildox-Alvarado, E., and J. Toro-Vazquez, Isothermal Crystallization of Tripalmitin in Sesame Oil, *Ibid*. *74*:69–76 (1997).
32. Metin, S., and R.W. Hartel, Thermal Analysis of Isothermal Crystallization Kinetics in Blends of Cocoa Butter with Milk Fat or Milk Fat Fractions, *Ibid. 75*:1617– 1624 (1998).
33. Kawamura, K., The DSC Thermal Analysis of Crystallization Behavior in Palm Oil, *Ibid*. *56*:753–758 (1979).
34. Christian, J.W., *The Theory of Transformations in Metals and Alloys; An Advanced Textbook in Physical Metallurgy*, Permagon Press, Oxford, London, 1965, pp. 16–22, 471–495.
35. Henderson, D.W., Thermal Analysis of Non-Isothermal Crystallization Kinetics in Glass Forming Liquids, *J. Non-Crystalline Solids 30*:301–315 (1979).
36. Graydon, J.W., S.J. Thorpe, and D.W. Kirk, Determination of the Avrami Exponent for Solid State Transformations from Non-Isothermal Differential Scanning Calorimetry, *Ibid*. *175*: 31–43 (1994).
37. Sharples, A., Overall Kinetics of Crystallization, in *Introduction to Polymer Crystallization*, edited by A. Sharples, Edward Arnold Ltd., London, 1966, pp. 44–59.
38. Strickland-Constable, R.F., Nucleation of Solids, in *Kinetics and Mechanism of Crystallization*, Academic Press, London, 1968, pp. 74–129.
39. Herrera, M.L., M. De Leon Gatti, and R.W. Hartel, A Kinetic Analysis of Crystallization of a Milk Fat Model System, *Food Res. Int. 32*:289–298 (1999).
40. Marangoni, A.G., and R.W. Hartel, Visualization and Structural Analysis of Fat Crystal Networks, *J. Food Technol*. *5*:46–51 (1998).
41. Bitman, J., and D.L. Wood, Changes in Milk Phospholipids During Lactation, *J. Dairy Sci. 73*:1208–1216 (1990).
42. National Dairy Council (NDC), *Newer Knowledge of Milk and Other Fluid Dairy Products*, NDC, Rosemont (1993).
43. van Grotenhuis, E., G.A. van Aken, K.F. van Malssen, and H. Schenk, Polymorphism of Milk Fat Studied by Differential Scanning Calorimetry and Real-Time X-ray Powder Diffraction, *J. Am. Oil Chem. Soc*. *76*:1031–1039 (1999).
44. Ng, W.L., A Study of the Kinetics of Nucleation in a Palm Oil Melt, *Ibid*. *67*:879–881 (1990).
45. Wang, F.S., and C.W. Lin, Turbidimetry for Crystalline Fractionation of Lard, *Ibid*. *72*:585–589 (1995).
46. Grall, D.S., and R.W. Hartel, Kinetics of Butterfat Crystallization, *Ibid*. *69*:741–747 (1992).
47. Sato, K., Crystallization Phenomena in Fats and Lipids, *J. Dispersion Sci. Technol. 10*:363–392 (1989).
48. Willis, W.M., and A.G. Marangoni, Assessment of Lipase- and Chemically Catalyzed Lipid Modification Strategies for the Production of Structured Lipids, *J. Am. Oil Chem. Soc*. *76*:443–450 (1999).
49. Herrera, M.L., C. Falabella, M. Melgarejo, and M.C. Añon, Isothermal Crystallization of Hydrogenated Sunflower Oil: I—Nucleation, *Ibid*. *75*:1273–1280 (1998).

[Received September 21, 1999; accepted February 6, 2000]